

See discussions, stats, and author profiles for this publication at: <https://www.researchgate.net/publication/265052962>

Determination of adsorbed species of hypophosphite electrooxidation on Ni electrode by in situ infrared with shell-isolated nanoparticle-enhanced Raman spectroscopy

ARTICLE *in* ELECTROCHEMISTRY COMMUNICATIONS · NOVEMBER 2014

Impact Factor: 4.85 · DOI: 10.1016/j.elecom.2014.08.002

CITATION

1

READS

71

10 AUTHORS, INCLUDING:



Liu-Bin Zhao

Southwest University in Chongqing

20 PUBLICATIONS 282 CITATIONS

SEE PROFILE



Wen-Bin Cai

Fudan University

111 PUBLICATIONS 2,067 CITATIONS

SEE PROFILE



Deyin Wu

Xiamen University

140 PUBLICATIONS 4,368 CITATIONS

SEE PROFILE



Zhong-Qun Tian

Xiamen University

354 PUBLICATIONS 9,823 CITATIONS

SEE PROFILE



Determination of adsorbed species of hypophosphite electrooxidation on Ni electrode by in situ infrared with shell-isolated nanoparticle-enhanced Raman spectroscopy

Yi-Feng Jiang^a, Bei Jiang^b, Li-Kun Yang^a, Meng Zhang^a, Liu-Bin Zhao^a, Fang-Zu Yang^{a,*}, Wen-Bin Cai^b, De-Yin Wu^a, Zhi-You Zhou^a, Zhong-Qun Tian^a

^a State key laboratory of physical chemistry of solid surfaces, Department of Chemistry, College of Chemistry and Chemical Engineering, Xiamen University, Xiamen 361005, China

^b Shanghai Key Laboratory of Molecular Catalysis and Innovative Materials, Collaborative Innovation Center of Chemistry for Energy Materials, Department of Chemistry, Fudan University, Shanghai 200433, China

ARTICLE INFO

Article history:

Received 4 July 2014

Received in revised form 1 August 2014

Accepted 4 August 2014

Available online 11 August 2014

Keywords:

Hypophosphite

Electrooxidation

Surface-enhanced infrared absorption spectroscopy

Shell-isolated nanoparticle-enhanced Raman spectroscopy

Adsorption orientation

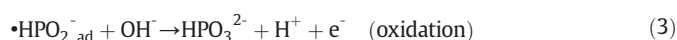
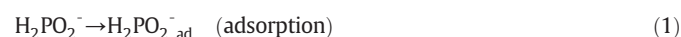
ABSTRACT

Electrooxidation of hypophosphite (H_2PO_2^-) on Ni electrode was investigated at the molecular level by external-reflection Fourier-transform infrared spectroscopy (FTIR), surface-enhanced infrared absorption spectroscopy with attenuated total reflection (ATR-SEIRAS), and shell-isolated nanoparticle-enhanced Raman spectroscopy (SHINERS). The results of external-reflection FTIR demonstrated that H_2PO_2^- could be oxidized to HPO_3^{2-} at significantly low potentials ($E < -1.0$ V vs. SCE). ATR-SEIRAS result showed that $\text{H}_2\text{PO}_2^-_{\text{ad}}$ could be adsorbed onto the Ni surface via O atoms. The adsorption orientation was further examined using SHINERS, and Ni-O stretching bands of metal-adsorbate vibration were directly detected. Comparative results of SHINERS and those obtained from the density functional theoretical calculation confirmed the adsorption orientation of H_2PO_2^- . The present investigation verified for the first time the adsorption mechanism of H_2PO_2^- electrooxidation on Ni surface through in situ spectroscopic data.

© 2014 Elsevier B.V. All rights reserved.

1. Introduction

Hypophosphite (H_2PO_2^-) is a well-known reducing agent for Ni electroless deposition [1,2], and Ni is known to be an excellent candidate catalyst for H_2PO_2^- oxidation. Therefore, spontaneous reduction of the Ni ion could be observed in Ni electroless deposition [3–5]. Numerous studies have been conducted to further understand the fundamental principles of the electrooxidation reaction of H_2PO_2^- on Ni surface [6–11]. The pioneering study suggests that the oxidation reaction for H_2PO_2^- involves three elementary processes, namely, adsorption, dehydrogenation, and oxidation.



Oliveira and Abrantes [6,7] suggested that $\text{H}_2\text{PO}_2^-_{\text{ad}}$ is adsorbed on the Ni surface through the H atoms. Zeng [10] and Cui [11] proposed an opposite adsorption orientation through density functional theory (DFT) calculation, in which $\text{H}_2\text{PO}_2^-_{\text{ad}}$ was adsorbed on the Ni surface via O atoms. However, limited experimental data have been obtained for determining the adsorption step of the H_2PO_2^- oxidation on the surface of Ni electrode. The detection and identification of the adsorbed species and adsorption orientation is essential to elucidate the H_2PO_2^- oxidation mechanism and precisely control Ni electroless deposition. These procedures are limited by the difficulty in studying the adsorbed species on Ni and their oxidation reactions using only traditional experimental approaches.

Surface-enhanced infrared (IR) absorption spectroscopy (SEIRAS) with attenuated total reflection (ATR) is a promising technique for investigating solid–liquid interfaces because of its high signal sensitivity and simple surface selection rule [12,13]. Shell-isolated nanoparticle-enhanced Raman spectroscopy (SHINERS) is a simple and cost-effective approach that expands the flexibility of surface-enhanced Raman scattering (SERS) for diverse applications in materials and

* Corresponding author. Tel.: +86 133 950 258 57.
E-mail address: fzyang@xmu.edu.cn (F.-Z. Yang).

surface sciences [14,15]. The results of the study on the electrooxidation reaction of H_2PO_2^- on Ni surface are presented by initially combining in situ FTIR, ATR-SEIRAS, and SHINERS.

2. Experimental

In situ FTIR measurements were carried out on a Nicolet-8700 FTIR spectrometer (Thermo Scientific, USA) equipped with a liquid-nitrogen-cooled MCT-A detector. A CaF_2 disk was used as IR window. The resulting spectrum is defined as $\Delta R/R = (R(\text{ES}) - R(\text{ER})) / R(\text{ER})$. A polycrystalline Ni disk was used as working electrode. A Pt foil was used as counter electrode, and a saturated calomel electrode (SCE) as a reference electrode.

A Varian 3100 FT-IR Excalibur Series spectrometer equipped with an MCT detector was used for ATR-FTIR measurements at incidence angles of 60 and 65 °C with a spectral resolution of 8 cm^{-1} , respectively. All the spectra are shown in the absorbance unit as $-\log(I/I_0)$. The Ni working electrode was formed according to the wet processes [16] on the reflecting plane of an ATR Si prism. An Au foil and a reversible hydrogen electrode (RHE) served as the counter and reference electrodes, respectively.

Raman spectra were recorded on an R1000 confocal microprobe Raman system (Renishaw, England). The excitation wavelength was 632.8 nm from a HeNe laser, and power on the sample was about 10 mW. A 50 \times magnification long working distance (8 mm) objective was used to focus the laser onto the sample and collect the scattered light in a backscattering geometry. A Pt wire and an SCE served as the counter and the reference electrodes, respectively. Au@SiO₂ NPs were assembled on the polished nickel electrode to form a layer of particles covering the electrode. The Au NPs were prepared according to the literature [17].

Density functional theory (DFT) calculations were carried out with the hybrid exchange-correlation functional B3LYP. The basis sets for P, O, and H atoms of investigated molecules were 6-311 + G(d, p). For Ni atoms, the valence electrons and the inner shells were described by the basis set, LANL2DZ, and the corresponding relativistic effective core potentials. The solvent effect was considered by integral equation formalism polarization continuum model (PCM) [18]. All calculations including structure optimization and vibrational spectra computation were carried out by using Gaussian 09 package [19].

3. Results and discussion

The transmission FTIR spectra of 0.3 M NaH_2PO_2 and 0.3 M Na_2HPO_3 are shown in Fig. 1A shows. No $\text{P}=\text{O}$ stretching band of H_2PO_2^- was detected, which should appear in the 1190 cm^{-1} to 1300 cm^{-1} range [20,21]. The absence of this peak indicates that the negative charge of the H_2PO_2^- is shared between the two equivalent P–O bonds rather than being restricted to one of the O atoms. In addition, a well-defined band at 1647 cm^{-1} is assigned to the bending mode of H_2O . The bands at 2349, 1160, 1088, and 1042 cm^{-1} could be assigned to $\nu(\text{P-H})$, $\nu_{\text{as}}(\text{O-P-O})$, $\omega(\text{H-P-H})$, and $\nu_{\text{s}}(\text{O-P-O})$ of H_2PO_2^- , respectively [22–24]. Moreover, the bands at 2323 and 1080 cm^{-1} are attributed to $\nu(\text{P-H})$ and $\nu_{\text{as}}(\text{PO}_3)$ of HPO_3^{2-} , respectively. Fig. 1B illustrates the in situ external-reflection FTIR spectra of Ni electrode in 0.03 M H_2PO_2^- at different sample potentials from –1.0 V to –0.40 V. The appearance of positive bands at 2349, 1160, and 1042 cm^{-1} and negative bands at 2323 and 1080 cm^{-1} at all potentials indicates the consumption of H_2PO_2^- and formation of HPO_3^{2-} , respectively. Therefore, HPO_3^{2-} can be regarded as the only oxidation product.

H_2PO_2^- adsorption is difficult to detect in the external-reflection FTIR spectra because of the overlapping bands from the free H_2PO_2^- in the solution. ATR-SEIRAS technique was used to detect the adsorbed species in the dilute H_2PO_2^- solution to minimize the effect of the bulk solution. In situ ATR-SEIRA spectra recorded during the electrooxidation of

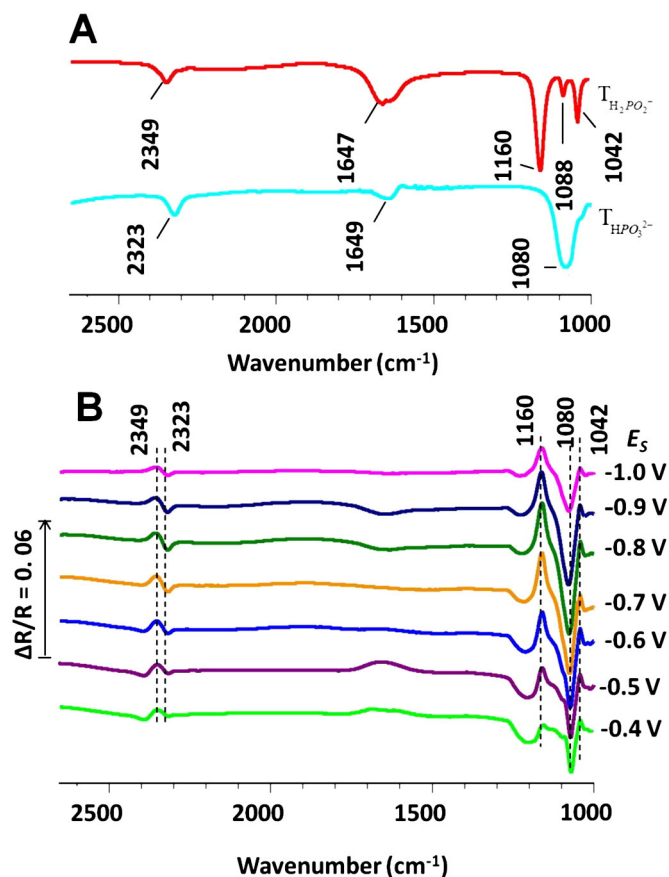


Fig. 1. (A) Transmission FTIR spectra of 0.3 M NaH_2PO_2 and 0.3 M Na_2HPO_3 , respectively. (B) In situ external-reflection FTIR spectra of Ni electrode in 0.03 M NaH_2PO_2 at different potentials varied from –1.0 to –0.40 V. $E_{\text{R}} = -1.2$ V. (For interpretation of the references to colour in this figure, the reader is referred to the web version of this article.)

0.03 M NaH_2PO_2 on Ni are shown in Fig. 2. The band at 1220 cm^{-1} could be attributed to the O–Si–O stretching of the silicon oxides formed (and/or grown) on the exposed Si sites, which is thermodynamically facilitated with increasing local pH upon H evolution [25]. Another possible candidate species for this band are the silicates formed at certain potentials [26]. A positive band at 1036 cm^{-1} to 1045 cm^{-1} appears at all potentials, which are attributed to O–P–O symmetrical stretching [22–24]. Moreover, the Stark tuning rate is evaluated to be 29.5 $\text{cm}^{-1} \text{V}^{-1}$ for $\nu_{\text{s}}(\text{O-P-O})$ on the Ni electrode. One possible explanation for the red shift observed in $\nu_{\text{s}}(\text{O-P-O})$ band with increasing electrode potential is the electron transfer effect. As the potential increases, the delocalized negative charge of H_2PO_2^- moves to the Ni electrode, which weakens the vibration of $\nu_{\text{s}}(\text{O-P-O})$. However, no other characteristic bands for $\nu_{\text{as}}(\text{O-P-O})$, $\nu(\text{H-P-H})$, and $\omega(\text{H-P-H})$ of H_2PO_2^- are observed. In the reflection IR spectroscopy, the surface selection rule [27] restricts that only vibrational modes with dipole component perpendicular to the metal surface are IR-active. The absence of $\nu_{\text{as}}(\text{O-P-O})$ suggests that H_2PO_2^- is adsorbed onto the Ni electrode surface via the two O atoms.

To complement the IR spectroscopic analysis, a set of potential-dependent SERS spectra of Ni in 0.03 M H_2PO_2^- were obtained, using the so-called SHINERS tactics (Fig. 3). Two clear bands at 280 and 412 cm^{-1} are observed at all potentials, which are assigned to the Ni–O stretching vibrations. The two bands are consistent with a metal-adsorbate vibration [$\nu_{\text{s}}(\text{O-Ni})$] although both bands are seldom observed on Ni electrodes in the literature. According to a previous report, the vibrational band corresponding to the Ni–O stretching mode of NiO_x film appears at a high frequency of 525 cm^{-1} [28]. Therefore, these two bands should originate from the metal-adsorbate vibrations rather than the metal oxide

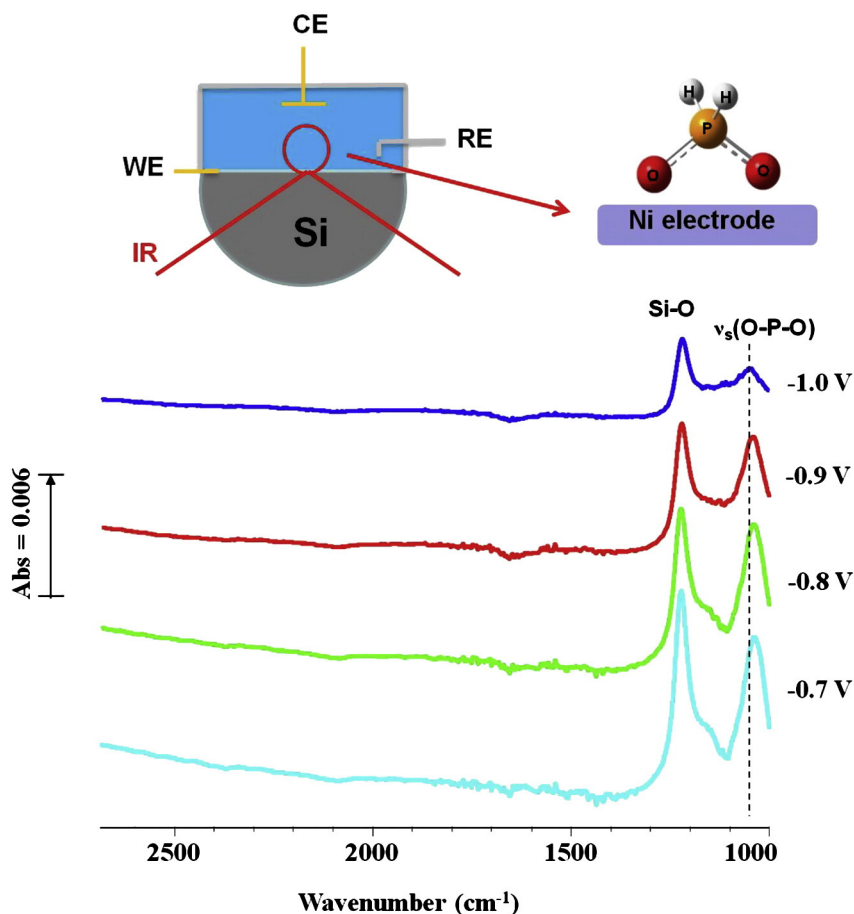


Fig. 2. In situ ATR-SEIRA spectra of nickel electrode in 0.03 M NaH_2PO_2 . $E_R = -1.2$ V. (For interpretation of the references to colour in this figure, the reader is referred to the web version of this article.)

film. To understand the observed Raman spectra, a DFT-simulated Raman spectrum for the interaction of H_2PO_2^- with a Ni cluster is also displayed in Fig. 3. The spectrum shows that the metal-adsorbate vibrational bands $\nu_s(\text{O-Ni})$ are assigned to 290 and 378 cm^{-1} . This predicted spectrum is in agreement with the observed spectra.

Based on the literature data and the above results, a consistent reaction mechanism of electrooxidation of H_2PO_2^- on Ni electrode is suggested in Scheme 1. This predicted pathway clearly elucidates the adsorption step of the electrooxidation process and the revised $\text{H}_2\text{PO}_2^-_{\text{ad}}$ adsorption orientation.

4. Conclusion

Crucial data for the adsorption of H_2PO_2^- electrooxidation on Ni electrodes were obtained from the in situ spectroscopic study. The adsorption orientation of H_2PO_2^- through two Ni-O bonds on Ni electrodes has been revealed for the first time by in situ ATR-SEIRAS and SHINERS. Thus, the electrooxidation of H_2PO_2^- undergoes an adsorption step and subsequently forms the final product HPO_3^{2-} .

Acknowledgment

This work was supported by the NSFC Innovation Group of Interfacial Electrochemistry (nos. 21373172 and 21321062).

References

- [1] T.R. Hendricks, E.E. Dams, S.T. Wensing, I. Lee, *Langmuir* 23 (2007) 7404.
- [2] T. Ouchi, Y. Arikawa, T. Homma, *J. Magn. Magn. Mater.* 320 (2008) 3104.
- [3] A. Brenner, G. Riddell, *J. Res. Natl. Bur. Stand.* 37 (1946) 31.
- [4] A. Brenner, G. Riddell, *J. Res. Natl. Bur. Stand.* 39 (1947) 385.
- [5] G. Gutzeit, *Plating* 46 (1959) 1158.
- [6] L.M. Abrantes, A. Bewick, M. Kalaji, M.C. Oliveira, *J. Chem. Soc. Faraday Trans.* 92 (1996) 4663.
- [7] L.M. Abrantes, M.C. Oliveira, J.P. Correia, A. Bewick, *J. Chem. Soc. Faraday Trans.* 93 (1997) 1119.
- [8] B. Jiang, M. Kunitomo, M. Yanagisawa, T. Homma, *J. Electrochem. Soc.* 160 (2013) 366.
- [9] Y. Zeng, Y. Zheng, S. Yu, K. Chen, S. Zhou, *Electrochem. Commun.* 4 (2002) 293.
- [10] Y. Zeng, L.H. Ou, Z.L. Li, X.M. Xiao, S.X. Xia, *Chinese J. Chem.* 25 (2007) 1246.
- [11] G.F. Cui, H. Liu, G. Wu, J.W. Zhao, S.Q. Song, P.K. Shen, *J. Phys. Chem. C* 112 (2008) 4601.
- [12] Y.X. Chen, A. Miki, S. Ye, H. Sakai, M. Osawa, *J. Am. Chem. Soc.* 125 (2003) 3680.
- [13] M.H. Shao, J. Warren, N.S. Marinkovic, P.W. Faguy, R.R. Adzic, *Electrochem. Commun.* 7 (2005) 459.
- [14] J.F. Li, Y.F. Huang, Y. Ding, Z.L. Yang, S.B. Li, X.S. Zhou, F.R. Fan, W. Zhang, Z.Y. Zhou, D.Y. Wu, B. Ren, Z.L. Wang, Z.Q. Tian, *Nature* 464 (2010) 392.
- [15] J.R. Anema, J.F. Li, Z.L. Yang, B. Ren, Z.Q. Tian, *Annu. Rev. Anal. Chem.* 4 (2011) 129.
- [16] J.Y. Wang, B. Peng, H.N. Xie, W.B. Cai, *Electrochim. Acta* 54 (2009) 1834.
- [17] Y.F. Huang, C.Y. Li, I. Broadwell, J.F. Li, D.Y. Wu, B. Ren, Z.Q. Tian, *Electrochim. Acta* 56 (2011) 10652.
- [18] J.B. Foresman, T.A. Keith, K.B. Wiberg, J. Snoonian, M.J. Frisch, *J. Phys. Chem.* 100 (1996) 16098.
- [19] M.J. Frisch, G.W. Trucks, H.B. Schlegel, G.E. Scuseria, M.A. Robb, J.R. Cheeseman, G. Scalmani, V. Barone, B. Mennucci, G.A. Petersson, H. Nakatsuji, M. Caricato, X. Li, H.P. Hratchian, A.F. Izmaylov, J. Bloino, G. Zheng, J.L. Sonnenberg, M. Hada, M. Ehara, K. Toyota, R. Fukuda, J. Hasegawa, M. Ishida, T. Nakajima, Y. Honda, O. Kitao, H. Nakai, T. Vreven, J.A. Montgomery Jr., J.E. Peralta, F. Ogliaro, M. Bearpark, J.J. Heyd, E. Brothers, K.N. Kudin, V.N. Staroverov, R. Kobayashi, J. Normand, K. Raghavachari, A. Rendell, J.C. Burant, S.S. Iyengar, J. Tomasi,

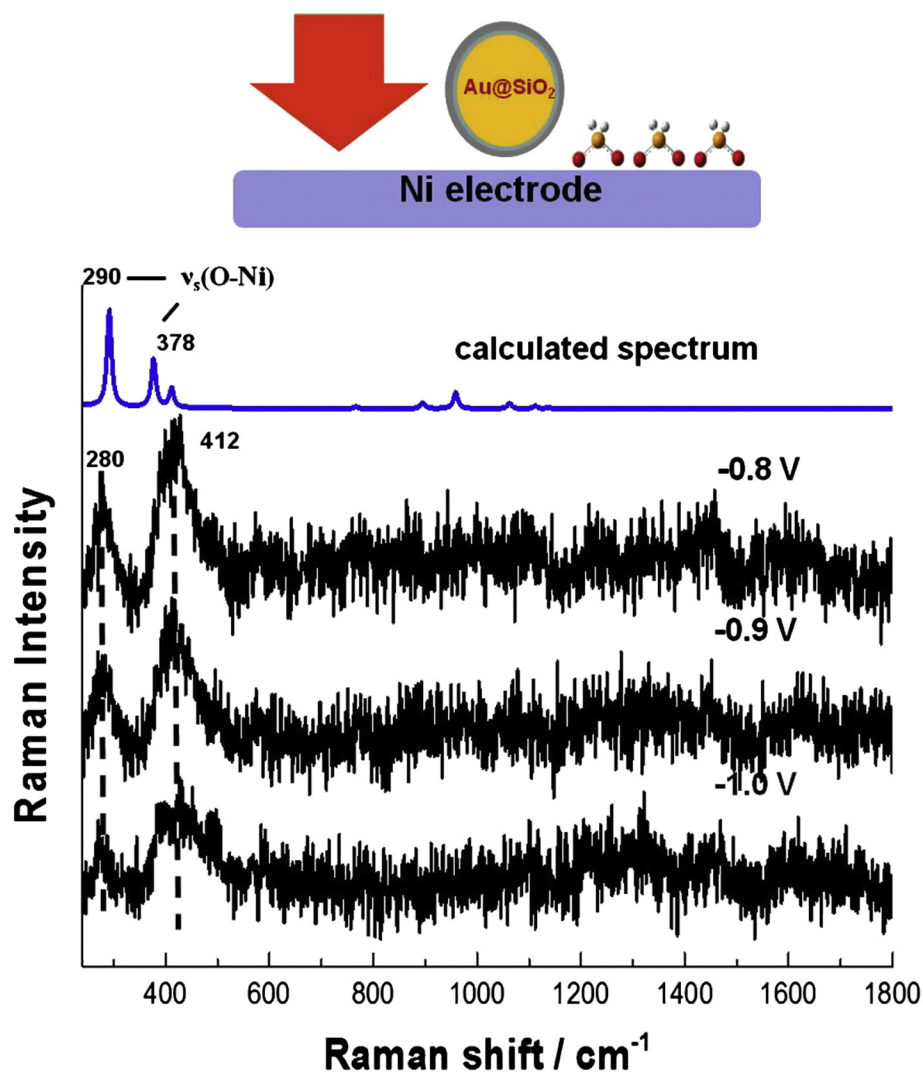
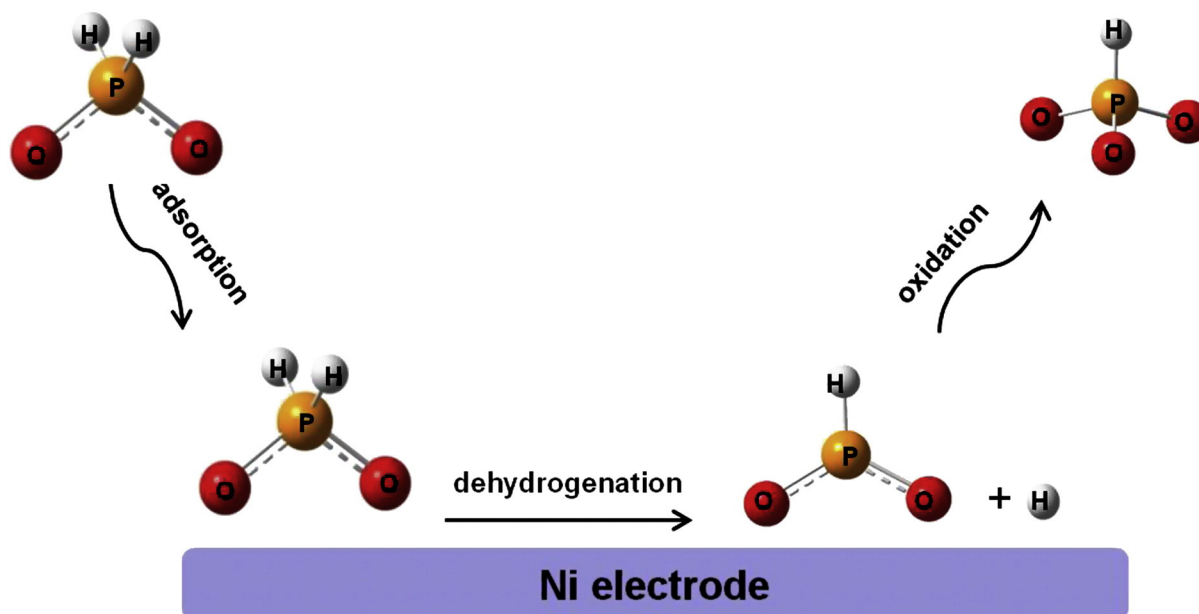


Fig. 3. Top: DFT calculated Raman spectra of H_2PO_2^- adsorbed on nickel electrode; lower three spectra: surface Raman spectra on a Ni electrode assembled with Au@SiO₂ NPs in 0.03 M NaH_2PO_2 solution. (For interpretation of the references to colour in this figure, the reader is referred to the web version of this article.)



Scheme 1. Reaction pathway for the electrooxidation of H_2PO_2^- on nickel surface.

- M. Cossi, N. Rega, J.M. Millam, M. Klene, J.E. Knox, J.B. Cross, V. Bakken, C. Adamo, J. Jaramillo, R. Gomperts, R.E. Stratmann, O. Yazyev, A.J. Austin, R. Cammi, C. Pomelli, J.W. Ochterski, R.L. Martin, K. Morokuma, V.G. Zakrzewski, G.A. Voth, P. Salvador, J.J. Dannenberg, S. Dapprich, A.D. Daniels, O. Farkas, J.B. Foresman, J.V. Ortiz, J. Cioslowski, D.J. Fox, et al., Gaussian 09, Revision A.02, Gaussian, Wallingford, CT, 2009.
- [20] L.C. Thomas, R.A. Chittenden, *Spectrochim. Acta* 20 (1964) 467.
- [21] L.C. Thomas, R.A. Chittenden, *Spectrochim. Acta* 26 (1970) 781.
- [22] M. Tsuboi, *J. Am. Chem. Soc.* 79 (1957) 1351.
- [23] J. Ziomek, J. Ferraro, D. Peppard, *J. Mol. Spectrosc.* 8 (1962) 212.
- [24] M. Abenoza, V. Tabacik, *J. Mol. Struct.* 26 (1975) 95.
- [25] V.P. Tolstoy, I.V. Chernyshova, V.A. Skrushevsky, *Handbook of Infrared Spectroscopy of Ultrathin Films*, John Wiley & Sons, New York, 2003.
- [26] H. Miyake, E. Hosono, M. Osawa, T. Okada, *Chem. Phys. Lett.* 428 (2006) 451.
- [27] M. Osawa, in: J.M. Chalmers, P.R. Griffiths (Eds.), *Handbook of Vibrational Spectroscopy*, John Wiley & Sons, Chichester, UK, 2002, p. 785.
- [28] S. Lee, H.M. Cheong, N. Park, C.E. Tracy, A. Mascarenhas, D.K. Benson, S.K. Deb, *Solid State Ionics* 140 (2001) 135.